Renewable Energy and Power Quality Journal
https://repqj.com/index.php/repqj/index
RE&PQJ, Vol. 23, No. 3, 2025

Ice Thickness Prediction and Risk Assessment of Transmission Lines Based on IQPSO-SVM

Yang Yang[1,2,*], Hongxia Wang[1,2], Meng Li[1,2], Shuyang Ma[1,2]

[1]State Grid Xinjiang Company Limited Electric Power Research Institute, Urumqi, 831000 Xinjiang, China
[2]Xinjiang Key Laboratory of Extreme Environment Operation and Testing Technology for Power Transmission & Transformation Equipment, Urumqi, 831000 Xinjiang, China
[*]Correspondence author's email: xjdky_yy@163.com

Abstract. In the TLs' ice thickness prediction, the position update of the traditional QPSO algorithm is easily affected by the average optimal position of the local attraction point particles, and the global search ability is poor, resulting in large ice thickness prediction errors, and the prediction of ice thickness of TLs and risk assessment cannot be combined. This paper used weighted coefficients, differential evolution operators and GA to improve the QPSO algorithm, used IQPSO to optimize the SVM parameters, and applied it to the prediction of ice thickness of TLs, combined with LSTM for risk assessment. The study used the grey correlation method to explore the influence of temperature, humidity, etc., on the TLs' ice thickness. Then, the differential evolution operator is used to improve the local attraction points, the weighted coefficient is introduced to improve the global optimal solution, and the crossover and mutation operator operations of GA are applied to QPSO to increase the diversity of solutions. Finally, the paper applied IQPSO to the SVM's kernel fuction width, output the optimal solution and the prediction rusult and evaluated the TLs' icing risk combined with LSTM. The results show that the IQPSO-SVM in this paper has the highest ice prediction accuracy, with a *MAPE* of 1.49%, which is 1.35% lower than that of QPSO-SVM, and the accuracy of the LSTM risk assessment model is as high as 0.97. The study shows that the IQPSO-SVM in this paper can achieve high-precision ice thickness prediction and combine it with LSTM to achieve accurate risk assessment performance.

Key words. Transmission Lines, Ice Thickness Prediction, Risk Assessment, Differential Evolution Operator, Crossover and Mutation

1. Introduction

TLs (Transmission lines) are often affected by ice and snow in winter, and icing occurs frequently. Especially in cold regions, icing on TLs can seriously threaten the safety of power facilities [1-3]. The thickness and distribution of icing directly affect the stability and carrying capacity of TLs, thus affecting the reliability of power supply [4-5]. Existing icing prediction methods such as QPSO-SVM (Quantum Particle Swarm Optimization-Support Vector Machine) face problems such as low prediction accuracy, poor model generalization ability, and risk assessment not combined with prediction. More advanced algorithms are urgently needed for optimization. To reduce power accidents caused by icing, accurately predicting the thickness of icing and conducting corresponding risk assessments have become important topics in power system research.

The study found that the LSTM model can to process time series data when conducting risk assessment and has been widely used in various prediction tasks. However, integrating LSTM into the risk assessment of TL ice thickness prediction still faces multiple challenges. The LSTM model has high requirements for the quality of input data, especially in long time series prediction, where noise and incomplete data will affect its performance. LSTM can process time series data, but it requires more computing resources and tuning when faced with complex nonlinear relationships and high-dimensional data. It is an important challenge to achieve accurate risk assessment in combining LSTM output with the actual risk assessment and transforming them into actionable decision suport effectively. Therefore, optimizing the LSTM model and improve its accuracy and usability in risk assessment has become one of the important goals of this study.

This paper aims to solve the limitations of the traditional QPSO algorithm in the prediction of ice thickness on TLs, especially its insufficiency in global search capability. This paper adopts an improved QPSO algorithm and optimizes the search strategy of the QPSO algorithm by introducing differential evolution operator, weighted coefficient and genetic algorithm (GA). The differential evolution operator is used to improve the local optimal solution, and the weighted coefficient and

GA crossover mutation operator enhance the diversity of solutions, further improving the global search capability. The experiment applies the IQPSO (Improved Quantum Particle Swarm Optimization) algorithm to the parameter optimization of SVM (Support Vector Machine), and combines the grey correlation method to analyze the influence of environmental factors such as temperature and humidity on ice thickness, so as to achieve high-precision prediction of ice thickness of TLs. The LSTM (Long Short-Term Memory) model is used to conduct risk assessment on the prediction results, achieving higher accuracy and prediction performance. This paper organically combines ice thickness prediction with risk assessment, and combines a new optimization algorithm to achieve relatively ideal prediction accuracy and risk assessment results.

Article Contribution:

(1) This paper innovatively introduces differential evolution operators, weighted coefficients and GA into the QPSO algorithm to improve the global search capability and solution diversity, effectively solve the local optimal problem of the traditional QPSO algorithm in ice thickness prediction, and improve the prediction accuracy significantly.

(2) The study applies IQPSO to SVM parameter optimization to improve the performance of SVM in ice thickness prediction, so that the model can more accurately predict the ice thickness of TLs and achieve significant performance improvement compared with traditional methods.

(3) This paper organically combines ice thickness prediction with risk assessment, uses LSTM for risk assessment, achieves high accuracy, and provides more accurate decision support for ice risk management of TLs.

2. Related Work

In TL ice thickness prediction, many scholars have used different prediction methods to conduct research. Hao et al. used flash infrared thermal imaging and BP (backpropagation) neural networks to predict ice thickness with an error of less than 0.1 [6]. Wang et al. used a combination of CNN (Convolutional Neural Networks) and BiGRU (Bidirectional Gated Recurrent Unit) models to predict the ice thickness of TLs, reducing the prediction error [7]. Ice detection based on infrared thermal imaging and equivalent ice thickness detection methods for overhead lines based on axial tension measurement have been applied, and it was found that the ice thickness detected by the method is consistent with the results caused by meteorological factors [8,9]. Ke, Yang and other scholars used the Transformer model and ACO-BPNN (Ant Colony Optimization-Back Propagation Neural Network) to predict the ice thickness of TLs and improve the accuracy of prediction [10,11]. Li et al. combined CNN and data mining technology to study the prediction of icing on power TLs, and also improved the prediction performance [12]. Wang et al. used an integrated model based on AI (Artificial Intelligence) to predict the thickness of icing on power TLs, with an error of less than 3 mm [13]. The above scholars used BP, Transformer, etc., to predict the thickness of ice, which reduced the prediction error to a certain extent, but the prediction error was not ideal.

Artificial intelligence technology has a good application in the risk assessment of TLs. Many scholars have applied artificial intelligence technology to risk assessment and achieved a lot of research results. Yang et al. used a TL dance reconstruction method based on dictionary learning to warn of geological disaster damage to TLs and improve the accuracy of warning level classification [14]. STAE-YOLO (Swin Transformer attention efficient algorithm-you only look once) and SVM-MLP (Support Vector Machine-Multilayer Perceptron) are widely used in TL risk management to improve the accuracy of risk assessment [15,16]. Shakiba et al. explored the application of machine learning methods in TL fault detection and risk assessment, revealing the importance of LSTM models in risk assessment accuracy [17]. Scholars applied artificial intelligence technology to the risk assessment of TLs and achieved good risk classification performance, but there is a large research gap in the risk assessment of ice thickness.

In recent years, methods combining optimization algorithms such as PSO (Particle Swarm Optimization) and SVM have been used and gradually applied to the prediction of ice thickness on TLs to improve the prediction accuracy. IAOA (Improved Arithmetic Optimization Algorithm) and IDBO (improved dung beetle optimizer) are widely used in LSSVM (least square support vector machine) parameter optimization and are applied to the prediction of ice thickness on TLs, greatly improving the prediction accuracy [18,19]. Song Yu and other scholars applied IPSO (improved Particle Swarm Optimization) to BP neural network optimization and improved the prediction accuracy of ice thickness [20]. Guo Kaichun and other scholars used PSO to optimize the performance of LSSVM in ice thickness prediction of TLs based on grey correlation weights and improved the prediction performance [21]. The study found that QPSO can better optimize the parameters of ARVM (adaptive relevance vector machine) and improve the fault probability prediction performance, but its search ability is poor [22]. The above scholars used PSO, IDBO, etc., to optimize the parameters of LSSVM, which improved the prediction accuracy of ice thickness on TLs. However, the global search ability was poor, which need optimization further.

LSTM and hybrid optimization algorithms have also achieved good application results in other studies. Shen Y et al. used a steady-state power quality risk warning method based on VMD-LSTM and fuzzy model to further improve the fault prediction accuracy of the

power system [23]. Yousaf M Z et al. used Bayesian optimization to optimize the LSTM-DWT model and achieved efficient fault detection in the MMC-based HVDC system [24]. Xu W et al. used the continuous PSO-GA algorithm to locate the fault of the distribution system and optimized the fault location accuracy of the system [25]. Guven A F et al. conducted a comparative study on the performance of the hybrid GA-PSO algorithm optimizing independent hybrid energy systems and provided new optimization ideas [26]. Scholars applied LSTM and hybrid optimization algorithms to other transmission line prediction and evaluation and achieved good results, which provided a solid research foundation for this article.

The improved IQPSO-SVM model used in this paper has significant differences and connections with existing studies. Compared with the BPNN used by Hao et al., the CNN and BiGRU model combined by Wang et al., and the ACO-BPNN used by Ke and Yang et al., the IQPSO-SVM model has made innovations in the optimization algorithm. They used differential evolution operators and weighted coefficients, and combines GA to enhance local and global search capabilities, thereby improving the prediction accuracy of the model. Compared with other studies using traditional PSO optimization, such as the use of IPSO to optimize BPNN by Song Yu et al., the IQPSO-SVM model has made breakthroughs in improving global search capabilities and avoiding falling into local optimal solutions. The improved algorithm in this paper effectively reduces the computational cost when processing large-scale data. Compared with the research using algorithms such as IDBO to optimize LSSVM, it can improve the computational efficiency of the model while ensuring high prediction accuracy. The improved model in this paper has a significant improvement in the optimization strategy and computational efficiency of the algorithm compared with existing methods. At the same time, it is consistent with the current research in the idea of combining machine learning and optimization algorithms, but it is innovative in the specific optimization scheme.

3. Ice Thickness Prediction Model for TLs

A. Construction of SVM Model

The regression equation output by SVM using nonlinear functions is shown in formula (1) [27,28].

$$g(x,\alpha)=(\alpha,\beta(z))+\gamma \quad (1)$$

α represents the weight vector and γ represents the bias.

In SVM, the objective function of the optimization problem is shown in formula (2).

$$\min\left\{0.5\|\alpha\|^2+\delta\sum_{i=1}^{n}(\eta_i+\eta_i')\right\} \quad (2)$$

δ represents the penalty coefficient and η_i represents the slack variable.

Based on the objective function of formula (2), the constraint condition is expressed as shown in formula (3).

$$\begin{cases}\theta_i-\alpha\cdot\beta(z)-\gamma\le\zeta+\eta_i\\ \alpha\cdot\beta(z)+\gamma-\theta_i\le\zeta+\eta_i'\end{cases} \quad (3)$$

ζ represents the error, and $\{z_i,\theta_i\}$ represents the sample size.

This paper introduces the sum kernel function and Lagrange multiplier, and formula (1) is transformed into formula (4).

$$g(z,\vartheta_{i,},\vartheta_i^1)=\sum_{i=1}^{n}(\vartheta_{i,},\vartheta_i^1)A(z,z_i)+\gamma \quad (4)$$

$A(z,z_i)$ represents the kernel function.

B. QPSO Algorithm

QPSO uses the principles of quantum mechanics to optimize the search behavior of particles [29-31]. In traditional PSO, particles update their positions based on their current positions and historical optimal positions, but QPSO introduces the concept of quantum bits, and implements the particle update mechanism through quantum superposition and quantum measurement, thereby enhancing the global search capability of particles. QPSO uses the probability distribution of quantum bits to determine the next position of particles, so that the algorithm can avoid falling into the local optimal solution and has stronger global exploration capabilities.

In the QPSO algorithm, it consists of multiple particles and multi-dimensional space. The position's particle is expressed as shown in formula (5).

$$Z_i=\{Z_{i1},Z_{i2},\cdots,Z_{iB}\} \quad (5)$$

B represents the dimension of space.

In quantum space, the position of particles is random. In practice, when the particles converge to their local attraction points, the algorithm converges. The expression of the local attraction point is shown in formula (6).

$$L_{ib} = \frac{\iota_1 \kappa_1 Q_{ib}(t) + \iota_2 \kappa_2 Q_{jb}(t)}{\iota_1 \kappa_1 + \iota_2 \kappa_2} \quad (6)$$

ι and κ represent random numbers. Q_i represents the optimal position of the particle, and Q_j represents the optimal position of the particle in the world.

The particle update expression is shown in formulas (7) and (8).

$$X_{ib}(t+1) = L_{ib} \pm \epsilon \left| \mathrm{mb}(t) - L_{ib}(t) \right| In\left(\frac{1}{\lambda}\right) \quad (7)$$

λ represents a random number and ϵ represents an innovation parameter.

$$L_i(t) = 2\epsilon \times \left| \mathrm{mb}(t) - L_{ib}(t) \right| \quad (8)$$

The calculation of $\mathrm{mb}(t)$ is shown in formula (9).

$$\mathrm{mb}(t) = \frac{1}{N} \sum_{i=1}^{N} Q_{ib}(t) \quad (9)$$

C. IQPSO Algorithm

1) Differential Evolution Operator

The traditional QPSO algorithm has the problem of insufficient global search ability and easy to fall into the local optimal solution in the prediction of ice thickness of transmission lines, resulting in low prediction accuracy. To improve the accuracy of prediction, this paper improves the QPSO algorithm by introducing differential evolution operator, weighted coefficient and GA. These improvements in this paper enhance the diversity and global search ability of particles, effectively avoid the trap of local optimal solution, and improve the optimization effect of the model. The IQPSO algorithm can more accurately optimize the SVM's parameters and achieve higher accuracy ice thickness prediction and risk assessment through using experimental method.

This paper introduces the differential evolution operator [32,33], weighted coefficient, and GA algorithm to improve the two parameters of L_{ib} and $\mathrm{mb}(t)$, enhance the global search capability.

Differential evolution is a population-based stochastic optimization algorithm that seeks the optimal solution to a problem by simulating the mutation process in natural selection and genetics [34,35]. In differential evolution, the algorithm generates new solutions by performing differential operations on individuals, corresponding to linear combinations of the differences between three random individuals in the selected population and the current solution of a target individual to generate new candidate solutions.

In the QPSO algorithm, if Q_j falls into Q_i, the diversity of the particle swarm can be reduced. In the particle swarm, two different particles are randomly selected. For particles o_1 and o_2, it is necessary to ensure that o_1, o_2 and i are not equal. The position difference calculation formula between particles is shown in formula (10).

$$\mu_{ib}(t) = z_{io_1}(t) - z_{io_2}(t) \quad (10)$$

$\mu_{ib}(t)$ represents position difference.

After the differential evolution operator is optimized, the calculation of the particle evolution expression is shown in formula (11).

$$Z_{ib}(t+1) = \mu_{ib}(t) \pm \epsilon \left| \mathrm{mb}(t) - Z_{ib}(t) \right| In\left(\frac{1}{\lambda}\right) \quad (11)$$

2) Weighted Coefficient

In the QPSO algorithm, each particle of $\mathrm{mb}(t)$ is equally divided, which is difficult to meet the actual situation. This paper sorts the particles according to their fitness and assigns weighted coefficients [36]. The calculation formula of the weighted coefficient is shown in formula (12).

$$\mathrm{mb}^1(t) = \sum_{i=1}^{N} \left(\frac{\nu \cdot Q_{ib}(t)}{N} \right) \quad (12)$$

ν represents the weight coefficient.

After introducing the weight coefficient optimization, the calculation of particle evolution expression is shown in formula (13).

$$Z_{ib}(t+1) = \mu_{ib}(t) \pm \epsilon \left| \mathrm{mb}^1(t) - Z_{ib}(t) \right| In\left(\frac{1}{\lambda}\right) \quad (13)$$

In formula (13), after introducing ν, this paper ensures that the particles are close to the optimal solution to a certain extent.

The calculation formula for updating the particle position is shown in formulas (14) and (15).

$$Q_{ib}(t)=\begin{cases}Z_{ib}(t) & g(Z_{ib}(t))<g(Q_{ib}(t-1)) \\ Q_{ib}(t-1) & \text{other}\end{cases} \quad (14)$$

$$Q_{j}(t)=\begin{cases}Q_{ib}(t) & g(Q_{ib})<g(Q_{j}(t-1)) \\ Q_{j}(t-1) & \text{other}\end{cases} \quad (15)$$

3) GA Algorithm

This paper introduces the GA algorithm [37,38] into the QPSO algorithm after weighted coefficient and differential evolution operator optimization to further enhance the global search capability and accelerate the convergence speed of particles. GA optimizes the particle swarm by simulating the natural selection, crossover and mutation processes of organisms, helping them overcome local optimal solutions and explore the entire solution space more effectively.

This paper first initializes the particle swarm, where each particle contains a set of positions and velocities.

Each generation of particles is selected according to the fitness value, and particles with high fitness have a greater probability of being selected to generate the next generation of particles. The selection of fitness function is shown in formula (16).

$$F_i=\frac{1}{1+R_i} \quad (16)$$

R_i represents the particle prediction error, and F_i represents the selection of the fitness function.

In the selection process of GA, this paper adopts the roulette selection method to select excellent individuals to participate in the reproduction of the next generation according to the fitness value of the individual. The probability function of roulette selection is shown in formula (17).

$$P_i=\frac{F_i}{\sum_{i=1}^{M}F_i} \quad (17)$$

P_i represents the probability of an individual being selected, and M represents the size of the population.

The selected particles generate new particles using the crossover operation, where the crossover operation generates new solutions by exchanging some positions or parameters between particles. The expression of particles is shown in formulas (18) and (19).

$$O_1=(x_1,z_1) \quad (18)$$

$$O_2=(x_2,z_2) \quad (19)$$

The crossover operation is expressed as shown in formulas (20) and (21).

$$P_{c1}=\left(\frac{x_1+x_2}{2},\frac{z_1+z_2}{2}\right) \quad (20)$$

$$P_{c2}=\left(\frac{x_1-x_2}{2},\frac{z_1-z_2}{2}\right) \quad (21)$$

After the crossover operation, the mutation operation further increases the diversity of solutions by slightly adjusting the genetic parameters of the particles. The formula for the mutation operation is shown in formula (22).

$$P_{\mathrm{m}}=P_{\mathrm{or}}+\varpi \quad (22)$$

ϖ represents the random perturbation amount.

The study uses the selection, crossover and mutation operations of GA to generate a new particle population and use it as the next generation particle population of QPSO. The partical population is continuously optimized to improve the global search capability through iteration.

D. Construction Process of IQPSO-SVM

The process of IQPSO-SVM is shown in Figure 1.

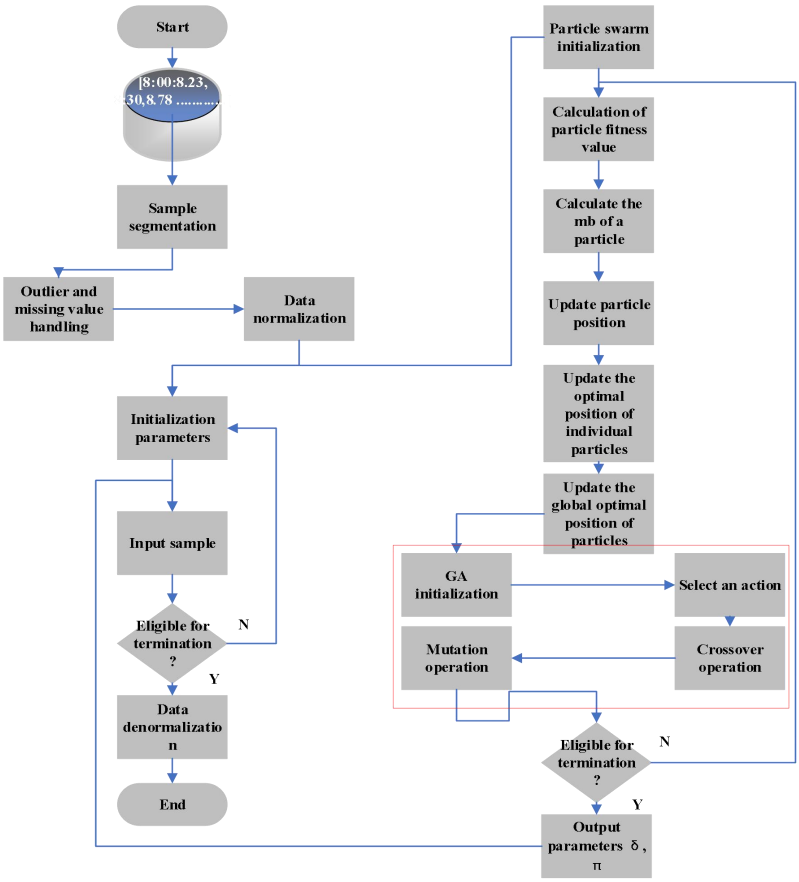

Figure 1. IQPSO-SVM process

In Figure 1, the process of IQPSO-SVM after the weighted coefficient, differential evolution operator, and GA algorithm are coordinated and optimized is as follows:

(1) Input the historical data of line ice coverage, perform sample segmentation, outlier and missing value processing, and normalization operations.

(2) Initialize the model parameters and calculate the particle fitness value.

(3) Use the differential evolution operator to enhance the global search capability, introduce the weighted coefficient to adjust the position distribution of particles through fitness, and use GA crossover mutation and other operations to further enhance the global exploration capability of the particle swarm to ensure the search for the global optimal solution.

(4) Calculate the average optimal position of the particles, and update the particle position after iteration, and output the solution of the penalty coefficient and kernel function width.

(5) Compare the fitness values and update the individual optimal position of the particle and the global optimal position of the particle.

(6) Refer to the termination condition to determine whether the termination requirements are met. If they are met, output the final solution of the penalty coefficient and kernel function width, otherwise continue to iterate.

4. Construction of LSTM Risk Assessment Model

In LSTM [39], the input layer of the model accepts the predicted ice thickness value optimized by IQPSO and some external environmental factors such as temperature and humidity as feature variables. The output layer is the risk assessment result, indicating the risk level corresponding to different ice thicknesses.

The forget gate is shown in formula (23).

$$\rho_t = \sigma\left(U_\rho\left[h_{t-1},\varphi_t\right]+\tau_\rho\right) \quad (23)$$

U_ρ and τ_ρ represent the weight matrix and bias term of the forget gate, respectively.

The input gate is shown in formula (24).

$$\varrho_t = \sigma\left(U\ \left[h_{t-1},\varphi_t\right]+\tau\ \right) \quad (24)$$

The candidate memory unit is shown in formula (25).

$$\tilde{D}_t = \tan\left(U_D\left[h_{t-1}, \varphi_t\right] + \tau_D\right) \quad (25)$$

The memory unit update is shown in formula (26).

$$D_t = \rho_t \cdot D_{t-1} + \varrho_t \cdot \tilde{D}_t \quad (26)$$

The output gate is shown in formula (27).

$$\varsigma_t = \sigma\left(U_\varsigma\left[h_{t-1}, \varphi_t\right] + \tau_\varsigma\right) \quad (27)$$

The hidden state is shown in formula (28).

$$h_t = \varsigma_t \cdot \tan h\left(D_t\right) \quad (28)$$

To map the LSTM output to a specific risk level, this paper uses a fully connected layer to further process the LSTM output and applies the softmax activation function to generate the probability distribution of risk assessment. The calculation of the probability distribution is shown in formula (29).

$$y_t = \text{soft max}\left(U_y \cdot h_t + \tau_y\right) \quad (29)$$

In model training,the loss function is expressed as shown in formula (30).

$$\text{Loss} = -\sum_{i=1}^{N} y_{t,i} \log\left(y_{p,i}\right) \quad (30)$$

The LSTM risk assessment model is shown in Figure 2.

In Figure 2, the ice thickness of the TL predicted by IQPSO-SVM and the environmental information are sent to LSTM for risk assessment, and the risk level of ice coverage of the TL is output.

This paper uses the Adam optimizer for parameter optimization and uses the dropout regularization technology for optimization.

The hyperparameter settings are shown in Table 1.

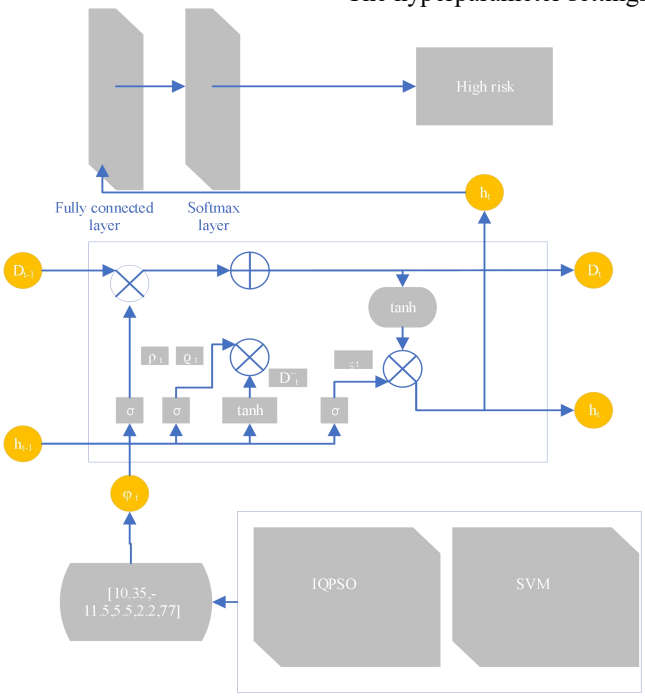

Figure 2. LSTM risk assessment model

Table 1. Hyperparameters

IQPSO-GA parameters	Value	LSTM parameters	Value
Maximum number of iterations	80	Number of input features	4
Population size	320	Number of LSTM units	64
Particle dimension	3	Number of time steps	10
Crossover percentage	0.7	Activation function	Tanh
Mutation percentage	0.5	Optimizer	Adam
Mutation rate	0.1	Learning rate	0.001
Selection pressure	8	Batch size	32
Gamma	0.2	Dropout ratio	0.2

In Table 1, the selection of the "mutation percentage" parameter is one of the key factors affecting performance improvement. The mutation operation can increase the diversity of solutions and prevent the algorithm from falling into the local optimal solution. By adjusting the mutation percentage, this paper can better explore the solution space and find a more optimized solution, making IQPSO more advantageous in global search and effectively improving the accuracy of the prediction model. The mutation operation plays a vital role in optimizing the performance of the model, especially in complex optimization problems.

5. Experimental Prediction and Risk Assessment of Ice Thickness of TLs

A. Experimental Data

The experimental data in this paper comes from the data of the monitoring department and meteorological department in Harbin, including historical data of ice thickness of TLs, temperature, humidity, wind speed, rainfall, air pressure, etc. The data collection time is from September to December 2023, and a total of 4225 sets of data are collected. To ensure the richness of the data, the experiment collected data from local monitoring departments and meteorological departments in Shenyang, Changchun, Urumqi, Tibet, Qinghai, Hohhot, and Baotou, and a total of 30,281 sets of data were collected. The experimental data of some ice thickness are shown in Table 2.

In Table 2, the ice thickness in Harbin during the day is mainly between 10-20 mm, which is in the medium ice zone, while at night the ice thickness reaches the heavy ice zone, corresponding to more than 20 mm.

The ice-covered image is shown in Figure 3.

Table 2. Experimental data of some ice thickness

Time	Ice thickness (mm)	Time	Ice thickness (mm)
8:00	8.23	14:30	18.45
8:30	8.78	15:00	19.02
9:00	9.15	15:30	19.85
9:30	9.5	16:00	20.3
10:00	10.02	16:30	21.1
10:30	10.48	17:00	21.75
11:00	11.12	17:30	22.5
11:30	11.8	18:00	23.1
12:00	12.55	18:30	23.8
12:30	13.1	19:00	24.25
13:00	13.5	19:30	24.95
13:30	14	20:00	25.5
14:00	14.6	-	

Figure 3. Ice-covered image

In Figure 3 the ice-covered state in Harbin's ice-covered area is very obvious and representative, which meets the actual needs of this article.

The visualization data of temperature, rainfall, humidity, and wind speed are shown in Figure 4.

In Figure 4, the rainfall is generally stable from 8:00 to 20:00 in a day, the temperature is relatively low in the morning and evening, and there is a certain fluctuation at noon, but it is always below 0 degrees. For wind speed, it is relatively stable overall. As humidity changes from morning to night, it is at its lowest value at about 16:00. The humidity percentage generally decreases first and then increases.

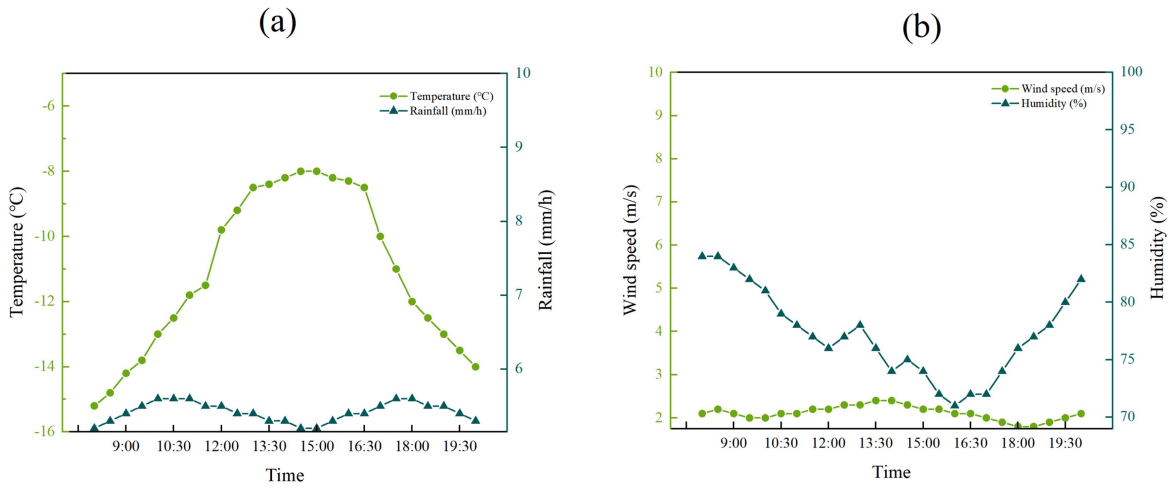

Figure 4. Visualization of data. Figure 4 (a) Visualization of temperature and rainfall; Figure 4 (b) Visualization of humidity and wind speed

B. Data Preprocessing

In the actual data collection process, some data may be missing due to sensor failure, data transmission interruption, etc. This paper uses linear interpolation to fill in the missing values. For outliers, this paper calculates the Z-Score of each data point. If the Z-Score is greater than 3 or less than -3, the data point is considered an outlier and replaced with the mean of the feature.

In the experiment, the dimensions and value ranges of multiple features vary greatly. This paper uses minimum-maximum normalization to scale the value of each feature to the interval $[0,1]$ for normalization.

C. Evaluation Indicators

MAPE (Mean Absolute Percentage Error):

$$MAPE = \frac{1}{n}\sum_{i=1}^{n}\left|\frac{\phi_i - \hat{\phi}_i}{\phi_i}\right| * 100\% \quad (31)$$

RMSE (Root Mean Square Error):

$$RMSE = \sqrt{\frac{1}{n}\sum_{i=1}^{n}\left(\phi_i - \hat{\phi}_i\right)^2} \quad (32)$$

6. Prediction Results of Ice Thickness of TLs

A. Grey Correlation Analysis

This paper uses grey correlation analysis to analyze the data of the monitoring department and meteorological department in Harbin, and the results are shown in Figure 5.

Grey correlation analysis helps identify which factors have a more significant impact on ice thickness by quantifying the correlation between environmental factors and ice thickness. The core role of this process is to provide a quantitative way to accurately quantify the relationship between multiple environmental variables and ice thickness, and provide more accurate input for the subsequent prediction model IQPSO-SVM. In this paper, grey correlation analysis can effectively improve the performance of the prediction model in this way, especially when considering the sensitivity of environmental factors to ice thickness prediction. Grey correlation analysis can also provide theoretical support for model selection, ensuring that the model can capture the most influential factors and further optimize the prediction accuracy.

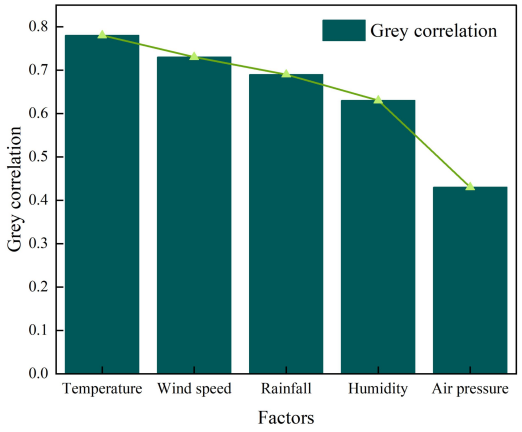

Figure 5. Correlation results

In Figure 5, temperature, wind speed, rainfall, humidity and ice thickness show strong correlation, while air pressure shows weak correlation. The correlations of temperature, wind speed, rainfall and humidity are 0.78, 0.73, 0.69 and 0.63 respectively, while the correlation of air pressure is only 0.43. It can be seen that the

correlation between temperature and ice thickness is the greatest.

B. Ice Thickness Prediction Performance of Different Models

The ice thickness prediction performance results of different models are shown in Figure 6. In Figure 6, the comparison models include SVM, PSO-SVM, QPSO-SVM, IQPSO (differential evolution operator)-SVM, IQPSO (differential evolution operator + weighted coefficient)-SVM, IQPSO (differential evolution operator + weighted coefficient + GA)-SVM.

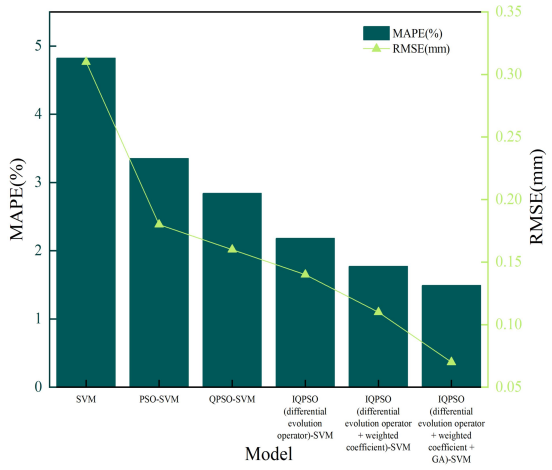

Figure 6. Ice thickness prediction performance of different models

In Figure 6, the *MAPE* of QPSO-SVM reaches 2.84% and the *RMSE* reaches 0.16mm. On the basis of QPSO-SVM, the differential evolution operator is introduced, reaching 2.18%, which is 0.66% lower than that of QPSO-SVM. The *RMSE* is only 0.14mm, which is 0.02mm lower than that of QPSO-SVM. This paper introduces the differential evolution operator and the weighted coefficient to optimize QPSO-SVM, and the *MAPE* reaches 1.77% and the *RMSE* reaches 0.11mm.

This paper introduces the differential evolution operator, weithted coefficient and GA algorithm and the *MAPE* reaches 1.49% based on QPSO-SVM, which is 1.35% lower than QPSO-SVM; the *RMSE* is only 0.07mm, which is 0.09mm lower than QPSO-SVM. In summary, the IQPSO (differential evolution operator + weighted coefficient + GA)-SVM ice thickness prediction model is the best, which is more suitable for ice thickness prediction of TLs.

C. Comprehensiveness Verification of the Model

To explore the comprehensiveness of the model, this paper takes the IQPSO (differential evolution operator + weighted coefficient + GA)-SVM ice thickness prediction model as the object, conducts experiments, and applies it to the ice thickness prediction in Shenyang, Changchun, Urumqi, Tibet, Qinghai, Hurhot, and Baotou. The results are shown in Table 3.

Table 3. Comprehensiveness verification results of the model

Region	*MAPE* (%)	*RMSE* (mm)	Region	*MAPE* (%)	*RMSE* (mm)
Harbin region	1.49	0.07	Tibet region	2.73	0.12
Shenyang region	1.89	0.09	Qinghai region	3.12	0.14
Changchun region	1.75	0.08	Hohhot region	2.1	0.1
Urumqi region	2.32	0.11	Baotou region	1.65	0.07

In Table 3, for *MAPE* , it is found that the *MAPE* in Shenyang, Changchun and Baotou is relatively low, ranging from 1.65% to 1.89%, and the prediction error of ice thickness is small. In Tibet, the *MAPE* reaches 2.73%, Qinghai reaches 3.12% and Urumqi reaches 2.32%, and the *MAPE* value is relatively high. It is precisely because the climatic conditions in these regions are more complex, the temperature difference is large, and the thickness of ice and snow in some areas is unevenly distributed, which affects the prediction accuracy of the model in these areas.

For *RMSE* , the Baotou area is smaller, and the model can effectively capture the changes in the actual ice thickness. The model reaches 0.12 mm in Tibet and 0.14 mm in Qinghai, and the *RMSE* is larger. The geographical environment in Tibet and Qinghai is complex, the altitude is high, and the climate fluctuates greatly, resulting in large differences in the distribution and thickness of ice and snow, affecting the prediction ability of the model. In summary, the model in this paper has differences in different regions, but the prediction error of ice thickness is low, which proves the comprehensiveness of the model.

D. Fitting Curve Analysis

The fitting curve is shown in Figure 7. In Figure 7, the horizontal axis is the number of iterations, and the vertical axis is the fitness value. The fitting curve includes QPSO, IQPSO (differential evolution operator), IQPSO (differential evolution operator + weighted coefficient), and IQPSO (differential evolution operator + weighted coefficient + GA).

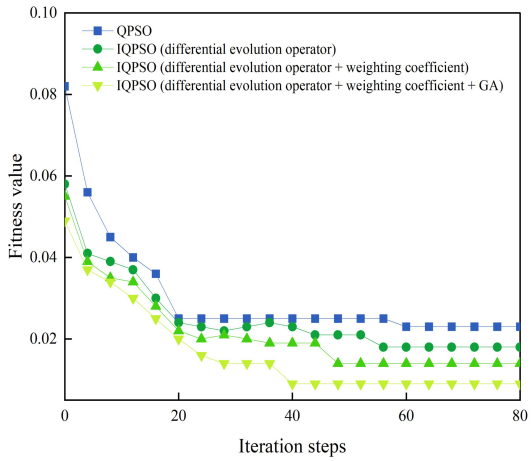

Figure 7. Fitting curve

In Figure 7, the QPSO algorithm tends to be stable after 20 and 60 iterations, and finds the global optimal solution, with fitness values of 0.025 and 0.023 respectively. IQPSO (differential evolution operator) continues to be stable after 44 and 56 iterations, and jumps out of the local optimal solution, with fitness values reaching 0.021 and 0.018 respectively. IQPSO (differential evolution operator + weighted coefficient) is relatively stable at iterations 36 and 48, and finds the global optimal solution, with fitness values of 0.019 and 0.014 respectively. IQPSO (differential evolution operator + weighted coefficient + GA) tends to be stable at iterations 28 and 40, with the best global convergence, and fitness values of 0.014 and 0.009 respectively.

E. Comparison Results with Other Hybrid Optimization Models

The comparison results with other hybrid optimization models are shown in Table 4. In Table 4, the compared optimization models include GA, ACO (Ant Colony Optimization), WOA (Whale Optimization Algorithm), SA (Simulated Annealing), ABC (Artificial Bee Colony), AOA (Arithmetic Optimization Algorithm), FOA (Fruit Fly Optimization Algorithm).

Table 4. Comparison results with other hybrid optimization models

Model	*MAPE* (%)	*RMSE* (mm)	Model	*MAPE* (%)	*RMSE* (mm)
IQPSO (differential evolution operator + weighted coefficient + GA)-SVM	1.49	0.07	SA-SVM	2.1	0.12
GA-SVM	2.35	0.15	ABC-SVM	2.2	0.13
ACO-SVM	2.5	0.17	AOA-SVM	2.6	0.18
WOA-SVM	2.15	0.11	FOA-SVM	2.3	0.14

In Table 4, the *MAPE* and *RMSE* values of the IQPSO-SVM model are 1.49% and 0.07 mm, respectively, which is the best performance, indicating that its prediction accuracy and precision are the highest. The *MAPE* and *RMSE* values of the GA-SVM, ACO-SVM, WOA-SVM and other models are relatively high, indicating that they are limited by their respective optimization strategies in the solution process, among which GA is more dependent on the initial population, and ACO has the problem of premature convergence in complex problems. AOA-SVM and FOA-SVM have the worst performance, with *MAPE* of 2.6% and 2.3%, and *RMSE* of 0.18 mm and 0.14 mm, respectively. Overall, the IQPSO-SVM model has an advantage in accuracy, while other algorithms are limited by different search mechanisms and convergence speeds, resulting in large prediction errors.

7. TL Icing Risk Assessment Results

A. Confusion Matrix

In the test set, there are 21 very low risk samples, 63 low risk samples, 106 medium risk samples, 148 high risk samples, and 85 very high risk samples. The confusion matrix is shown in Figure 8.

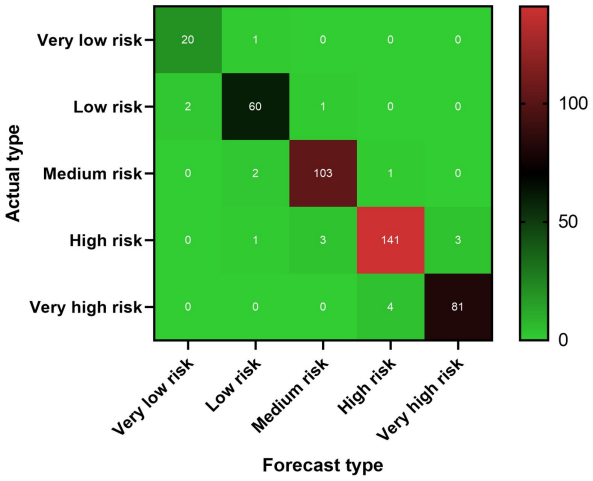

Figure 8. Confusion Matrix

In Figure 8, 20 samples of the extremely low risk type were correctly identified, and 1 sample was misidentified as low risk. 60 samples of the low risk type were correctly identified, 103 samples of the medium risk type were correctly identified, and 141 samples of the high risk type were correctly identified. Among the very high risk type samples, 81 were correctly identified, and 4 were misidentified as high risk. Overall, the risk assessment performance of the LSTM model is good.

B. TL Icing Risk Assessment Performance

The TL icing risk assessment results are shown in Figure 9. In Figure 9, the comparison models include GRU (Gate Recurrent Unit), XGBoost (Extreme Gradient Boosting), RF (Random Forest), and SVM.

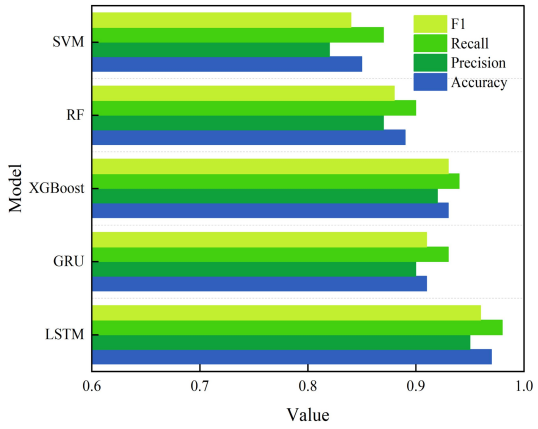

Figure 9. TL icing risk assessment results

In Figure 9, the LSTM model has the highest accuracy, reaching 0.97, and the F1 value reaches 0.96, indicating that LSTM can correctly classify most samples, especially the very low risk and very high risk categories. The SVM model has an accuracy of only 0.85, the worst performance. The accuracy of the GRU and XGBoost models are 0.91 and 0.93 respectively, the accuracy of RF is 0.89, and the F1 is 0.88.

Regarding precision and recall, LSTM has a clear advantage with precision and recall reaching 0.95 and 0.98 respectively. The precision of the SVM model is 0.82 and the recall is 0.87. The precision of GRU and XGBoost models are 0.9 and 0.92 respectively, and the recall rates are 0.93 and 0.94 respectively. In summary, LSTM achieves the best performance in the risk assessment of icing on TLs, which meets the actual needs.

8. Further Discussion

The LSTM model performs well in both TL icing risk assessment and icing thickness prediction. Its advantages mainly lie in its deep learning architecture and powerful modeling capabilities for time series data. In icing thickness prediction, LSTM can better capture the changing trend of icing by learning the long-term and short-term dependencies of time series, thus significantly improving the prediction accuracy. Based on the use of IQPSO to optimize the SVM model, this paper introduces differential evolution operators, weighted coefficients and GA to improve the stability and global convergence of the prediction results, making the IQPSO (differential evolution operator + weighted coefficient + GA)-SVM model the best in predicting ice thickness. The introduction of the optimization algorithm significantly improves the model's ability to learn complex patterns and further improves the prediction accuracy.

The IQPSO algorithm significantly enhances the global search capability and convergence speed by introducing differential evolution operators, weighted coefficients and GA to optimize the QPSO algorithm. Compared with the standard QPSO, IQPSO has higher computational complexity. The IQPSO needs to perform more operation to update particles's position and fitness after introducing differential evolution operatiors and genetic algorithms. The introduction of differential evolution and GA requires operations such as crossover and mutation in each iteration, which increases the computational burden of each particle. The computational complexity of IQPSO is higher than that of QPSO and PSO, especially when the particle swarm is large, its computing resources and time consumption increase significantly.

The scalability of IQPSO is better than that of the standard PSO and QPSO models. In IQPSO, the combined optimization of weighted coefficients, differential evolution operators and genetic algorithms improves the global search capability, enhances the diversity of solutions, effectively avoids falling into the local optimal solution, and makes IQPSO more adaptable when dealing with larger and more complex problems. Compared with standard PSO and QPSO, IQPSO can maintain better performance in a larger dimensional search space and is suitable for high-dimensional, complex constraints and multi-modal optimization problems. IOPSO can improce the solutions diversity and enhance scalability and robustness in different optimization tasks by introducing GA's crossover and mutation operations.

The results of this study have important practical significance and theoretical value in many aspects. This paper introduces LSTM and its optimization algorithm, which can efficiently process TL data with complex time series dependencies and multi-dimensional features, greatly improving the accuracy of ice thickness prediction. This is crucial for power companies and relevant regulatory authorities to timely grasp the health status of TLs and formulate reasonable operation and maintenance strategies. The various optimization algorithms used in this paper can provide better solutions when dealing with complex nonlinear problems, and provide new ideas and methods for the application of machine learning and optimization algorithms in practical engineering. The performance of various models in ice thickness prediction and risk assessment tasks is compared, which provides reference and reference for future research on similar problems.

The model used in this paper performed well in the experiment, but there are still the following limitations and future improvement directions.

(1) The data in this paper only come from the monitoring

and meteorological departments in Harbin, and the sample size is 4225 groups. Geographical regions are particular, and the icing conditions of TLs in other regions may be different. Future research can expand the data source, including data from more different regions and under different climate conditions.

(2) The IQPSO (differential evolution operator + weighted coefficient + GA)-SVM model showed good performance in this study, but its optimization algorithm can still be further improved. When processing large-scale data sets, existing algorithms can face problems with computing time and resource consumption. In the future, this paper can explore more efficient optimization algorithms or combine deep learning and reinforcement learning methods.

(3) This study mainly considers the impact of meteorological factors on ice thickness, but in actual situations, other factors such as power grid operation status and equipment aging can also affect ice thickness.

(4)The IQPSO model performs well in current experiments, but its computational cost remains a challenge in large-scale data processing and real-time prediction applications. The computational complexity of the IQPSO algorithm is high, especially in multidimensional data space, which will lead to a significant increase in computing time and resources. Future research will explore the following strategies: on the one hand, the computational efficiency can be improved through algorithm parallelization, distributed computing or GPU acceleration; on the other hand, the dimension of input data can be reduced as much as possible through feature selection and dimensionality reduction technology to reduce the computational burden.

9. Conclusions

This paper adopts a TL ice thickness prediction method based on IQPSO-SVM, using differential evolution operator, weighted coefficient and GA improved QPSO algorithm to improve the global search capability and optimize the parameters of the SVM model. The study uses the grey correlation method to analyze the impact of environmental factors such as temperature and humidity on ice thickness, and combines the LSTM model for risk assessment. The test results show that the IQPSO-SVM model greatly improves the prediction accuracy, and the LSTM model achieves good risk assessment accuracy. This paper has made some achievements, but there are some shortcomings. The experimental data only comes from the monitoring and meteorological departments in Harbin, the data diversity is limited, and the convergence performance needs to be further optimized. In the future, other improved advanced algorithms can be combined with the risk assessment model, and data from multiple regions can be collected to conduct experiments to further improve prediction accuracy and generalization.

Acknowledgment

None

Consent to Publish

The manuscript has neither been previously published nor is under consideration by any other journal. The authors have all approved the content of the paper.

Funding

State Grid Xinjiang Electric Power Co., Ltd. Science and Technology Projects, (No. 5230DK230005).

Author Contribution

[Yang Yang]: Developed and planned the study, performed experiments, and interpreted results. Edited and refined the manuscript with a focus on critical intellectual contributions.

[Hongxia Wang, Meng Li]: Participated in collecting, assessing, and interpreting the date. Made significant contributions to date interpretation and manuscript preparation.

[Shuyang Ma]: Provided substantial intellectual input during the drafting and revision of the manuscript.

Conflicts of Interest

The authors declare that they have no financial conflicts of interest.

References

[1] X.S. Dong, Y.H. Wan, Y.R. Zhang, Y.C. Zhu. Phase Risk Analysis of Overhead Lines Under Complex Icing Conditions. Applied Sciences, 2024, 14(22), 10701. DOI: 10.3390/app142210701

[2] B. Li, J. Bai, J.H. He, C. Ding, X. Dai, et al. A review on superhydrophobic surface with anti-icing properties in overhead transmission lines. Coatings, 2023, 13(2), 301-325. DOI: 10.3390/coatings13020301

[3] S. He, Y.H. Song, H.Y. Huang, Y.H. He, S.H. Zhou, et al. Meteorological Characteristics of a Continuous Ice-Covered Event on Ultra-High Voltage Transmission Lines in Yunnan Region in 2021. Atmosphere, 2024, 15(4), 389-405. DOI: 10.3390/atmos15040389

[4] Z.J. Zhang, H. Zhang, S. Yue, W.H. Zeng. A review of icing and anti-icing technology for transmission lines. Energies, 2023, 16(2), 601-631. DOI: 10.3390/en16020601

[5] L. Tan, Y. Liu, Z.H. Yuan, R. Li. Linear modeling analysis of the heat balance of the transmission line in high frequency critical ice melting state. International Journal of Low-Carbon Technologies, 2024, 19(1), 508-516. DOI: 10.1093/ijlct/ctad134

[6] L. Hao, Q.Y. Li, W.C. Pan, R. Yao, S.Y. Liu. Ice accretion thickness prediction using flash infrared thermal imaging

and BP neural networks. IET Image Processing, 2023, 17(3), 649-659. DOI: 10.1049/ipr2.12662

[7] F. Wang, H.B. Lin, Z.M. Ma. Transmission Line Icing Prediction Based on Dynamic Time Warping and Conductor Operating Parameters. Energies, 2024, 17(4), 945-958. DOI: 10.3390/en17040945

[8] L. Yang, Y.F. Chen, Y.P. Hao, L.C. Li, H. Li, et al. Detection method for equivalent ice thickness of 500-kV overhead lines based on axial tension measurement and its application. IEEE Transactions on Instrumentation and Measurement, 2023, 72(1), 1-11. DOI: 10.1109/TIM.2023.3264035

[9] A. Yousuf, H. Khawaja, M.S. Virk. Conceptual design of cost-effective ice detection system based on infrared thermography. Cold Regions Science and Technology, 2023, 215(1), 103941. DOI: 10.1016/j.coldregions.2023.103941

[10] H.C. Ke, H.B. Sun, H.L. Zhao, T. Wu. Ice Cover Prediction for Transmission Lines Based on Feature Extraction and an Improved Transformer Scheme. Electronics, 2024, 13(12), 2339-2343. DOI: 10.3390/electronics13122339

[11] L. Yang, L.L. Mei, Y.F. Chen, Y.P. Hao, L.C. Li, et al. Prediction Method for Mechanical Characteristic Parameters of Weak Components of 110 kV Transmission Tower under Ice-Covered Condition Based on Finite Element Simulation and Machine Learning. Machines, 2024, 12(9), 652-672. DOI: 10.3390/machines12090652

[12] L.X. Li, D. Luo, W.H. Yao. Analysis of transmission line icing prediction based on CNN and data mining technology. Soft Computing, 2022, 26(16), 7865-7870. DOI: 10.1007/s00500-022-06812-7

[13] G.Y. Wang, J. Shen, M.H. Jin, S. Huang, Z. Li, et al. Prediction model for transmission line icing based on data assimilation and model integration. Frontiers in Environmental Science, 2024, 12(1), 1-15. DOI: 10.3389/fenvs.2024.1403426

[14] Y. Yang, X.Q. Zhu, X. Song, H.H. Zhang, X. Zhang. Early warning and decision-making model of geological disaster damage of transmission lines based on intelligent online monitoring technology. International Journal of Information and Communication Technology, 2024, 24(7), 65-89. DOI: 10.1504/IJICT.2024.139109

[15] C. Ji, F. Zhang, X. B. Huang, Z.W. Song, W. Hou, et al. STAE-YOLO, Intelligent detection algorithm for risk management of construction machinery intrusion on transmission lines based on visual perception. IET Generation, Transmission & Distribution, 2024, 18(3), 542-567. DOI: 10.1049/gtd2.13093

[16] S. Behilil, M. Hendel, I.S. Bousmaha, K. Kessairi, M. Brahami. A new intelligent scheme for short-circuit detection, classification and location in power transmission lines with the PV generation presence. Studies in Engineering and Exact Sciences, 2024, 5(1), 2747-2773. DOI: 10.54021/seesv5n1-136

[17] F.M. Shakiba, S.M. Azizi, M.C. Zhou, Abusorrah A. Application of machine learning methods in fault detection and classification of power transmission lines, a survey. Artificial Intelligence Review, 2023, 56(7), 5799-5836. DOI: 10.1007/s10462-022-10296-0

[18] Tu Jinglin, Wang Hongliang. Research on prediction of ice thickness of transmission lines based on IAOA-LSSVM. Modern Electronic Technology, 2024, 47(21), 113-118. DOI: 10.16652/j.issn.1004-373x.2024.21.018

[19] Chen Jing, Li Ronghao. Prediction model of ice thickness of transmission lines based on IDBO-LSSVM. Journal of Hubei University for Nationalities (Natural Science Edition),2024,42(03),343-348. DOI: 10.13501/j.cnki.42-1908/n.2024.09.005

[20] Song Yu. Transmission line ice thickness prediction algorithm based on IPSO optimized BP neural network. Science and Technology Wind, 2022, 10(29), 1-3. DOI: 10.19392/j.cnki.1671-7341.202229001

[21] Guo Kaichun, Wang Bo. PSO-LSSVM transmission line ice thickness prediction model considering grey correlation weight. Electrical Materials,2022,4(1),15-19. DOI: 10.16786/j.cnki.1671-8887.eem.2022.01.004

[22] J. Zhao, H.X. Zhang, H.L. Zou, J.G. Pan, C.S. Zeng, et al. Probability prediction method of transmission line icing fault based on adaptive relevance vector machine. Energy Reports, 2022, 8(1), 1568-1577. DOI: 10.1016/j.egyr.2022.02.018

[23] Y. Shen, W. Hu, M.Q. Dong, F. Yang, Z.C. Yang, et al. A risk warning method for steady-state power quality based on VMD-LSTM and fuzzy model. Heliyon, 2024, 10(9), e30597. DOI: 10.1016/j.heliyon.2024.e30597

[24] M.Z. Yousaf, A.R. Singh, S. Khalid, M. Bajaj, B.H. Kumar, et al. Bayesian-optimized LSTM-DWT approach for reliable fault detection in MMC-based HVDC systems. Scientific Reports, 2024, 14(1), 17968. DOI: 10.1038/s41598-024-68985-5

[25] W.Z. Xu, J.C. Li, L. Yang, Q. Yu. Faults locating of power distribution systems based on successive PSO-GA algorithm. Scientific Reports, 2024, 14(1), 11259. DOI: 10.1038/s41598-024-61306-w

[26] A.F. Guven, N. Yorukeren. A comparative study on hybrid GA-PSO performance for stand-alone hybrid energy systems optimization. Sigma Journal of Engineering and Natural Sciences, 2024, 42(6), 1410-1438. DOI: 10.14744/sigma.2024.00108

[27] X.X. Gong, Y.Z. Zhu, Y.H. Wang, E.Y. Li, Y.H. Zhang, et al. Safety Status Prediction Model of Transmission Tower Based on Improved Coati Optimization-Based Support Vector Machine. Buildings, 2024, 14(12), 3815-3836. DOI: 10.3390/buildings14123815

[28] R. Zhou, Z.G. Zhang, T. Zhai, X.L. Gu, H.R. Cao, et al,. Machine learning-based ice detection approach for power transmission lines by utilizing FBG micro-meteorological sensors. Optics Express, 2023, 31(3), 4080-4093. DOI: 10.1364/OE.477309

[29] J.W. Bai, P.J. Cong, H. Zhang, S.X. Sun, B.W. Zhang, et al. Analysis of SF6 contact based on QPSO-SVR. Energy Reports, 2023, 9(1), 425-433. DOI: 10.1016/j.egyr.2023.03.020

[30] X. Liu, M. Liu, H. Yin. Application of QPSO-BPSO in fault self-healing of distributed power distribution networks. Energy Informatics, 2024, 7(1), 53-71. DOI: 10.1186/s42162-024-00358-8

[31] Z.G. Yan, M. Cui, X. Ma, J.R. Wang, Z.H. Zhang, et al. OPGW State Evaluation Method Based on MSIF and QPSO-DQN in Icing Scenarios. International Journal of Information Technologies and Systems Approach (IJITSA), 2024, 17(1), 1-26. DOI: 10.4018/IJITSA.343318

[32] R.P. Parouha, P. Verma. A systematic overview of developments in differential evolution and particle swarm optimization with their advanced suggestion. Applied Intelligence, 2022, 52(9), 10448-10492. DOI: 10.1007/s10489-021-02803-7

[33] K.M. Sallam, A.A. Abohany, R.M. Rizk-Allah. An enhanced multi-operator differential evolution algorithm for tackling knapsack optimization problem. Neural Computing and Applications, 2023, 35(18), 13359-13386. DOI: 10.1007/s00521-023-08358-7

[34] S. Chanda, S. Maity, A. De. A differential evolution modified quantum PSO algorithm for social welfare maximisation in smart grids considering demand response and renewable generation. Microsystem Technologies, 2022, 30(12), 1519-1536. DOI:

10.1007/s00542-022-05399-1
[35] M. Akhtar, A.K. Manna, A. Duary, A.K. Bhunia. A hybrid tournament differential evolution algorithm for solving optimisation problems and applications. International Journal of Operational Research, 2022, 45(3), 300-343. DOI: 10.1504/IJOR.2022.127140
[36] V.S. Rugveth, K. Khatter. Sensitivity analysis on Gaussian quantum-behaved particle swarm optimization control parameters. Soft Computing, 2023, 27(13), 8759-8774. DOI: 10.1007/s00500-023-08011-4
[37] R.X. Huang, X.F. Fu, Y.F. Pu. A novel fractional accumulative grey model with GA-PSO optimizer and its application. Sensors, 2023, 23(2), 636-650. DOI: 10.3390/s23020636
[38] Y.S. Yun, M. Gen, T.N. Erdene. Applying GA-PSO-TLBO approach to engineering optimization problems. Mathematical Biosciences and Engineering, 2023, 20(1), 552-571. DOI: 10.3934/mbe.2023025
[39] K.K. Xu, J.Q. Hu, L.B. Zhang, Y.Y. Chen, S.R. Xiao, et al. A risk factor tracing method for LNG receiving terminals based on GAT and a bidirectional LSTM network. Process Safety and Environmental Protection, 2023, 170(1), 694-708. DOI: 10.1016/j.psep.2022.12.047